STELLAR SPECTRA
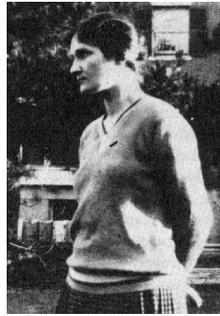
A. Basic Line Formation

R.J. Rutten

Sterrekundig Instituut Utrecht

February 6, 2007

Contents

Text available at \tthttp://www.astro.uu.nl/~rutten/education/rjr-material/ssa
(or via "Rob Rutten" in Google).

Introduction

These three exercises concern the appearance and nature of spectral lines in stellar spectra. Stellar spectrometry laid the foundation of astrophysics in the hands of:

- Wollaston (1802): first observation of spectral lines in sunlight;

- Fraunhofer (1814–1823): rediscovery of spectral lines in sunlight ("Fraunhofer lines"); their first systematic inventory. Also discussions of the spectra of Venus and some stars;

- Herschel (1823): realization that spectral lines must provide information on the constitution of stellar matter;

- Kirchhoff & Bunsen (1860): absorption lines in stellar spectra are the reverse of emission lines from the same particle species in laboratory flames. The strength of the absorption is a measure of the concentration of the species (abundance);

- Pickering plus "harem" (Williamina Fleming, Antonia Maury, Annie Cannon, and a dozen other women): large-scale spectral classification using photographic spectrograms taken with objective prisms. Annie Cannon classifies over 200 000 spectrograms and fine-tunes the Harvard spectral classification sequence O – B – A – F – G – K – M. This is a purely morphological division on the basis of spectral line appearances;

- Hertzsprung (1908) and Russell (1913) independently plot a diagram of stellar absolute magnitude against spectral type (Figure 1). It shows that stars occupy sharply defined locations in this parameter space;

- Cecilia Payne (1925): demonstration that the Saha ionization law explains stellar line strength variations. The Harvard spectral sequence is simply a measure of temperature. All stars have about the same chemical composition — not significantly different from the earth's composition apart from hydrogen)[1];

- Morgan (1938): introduction of the luminosity classification I – II – III – IV – V. This is "the other axis" of the empirical HRD, roughly orthogonal to the main sequence;

- Minnaert and coworkers (1930–1965, Utrecht): introduction of the equivalent width of a line and the curve of growth for quantitative abundance determination. Detailed inventory of the solar spectrum, first graphically in the "Utrecht Atlas" (Minnaert *et al.* 1940), then in tabular form in "The Solar Spectrum 2935Å– 8770Å" (Moore *et al.* 1966), listing equivalent widths for 24 000 Fraunhofer lines;

- Unsöld and coworkers (1940-1970, Kiel): precise stellar abundance determinations using LTE (Local Thermodynamic Equilibrium) modeling;

- Schwarzschild, Eddington, Milne, Thomas and many others throughout the twentieth century: development of more general line-formation theory, especially radiation transport through resonance scattering;

- Avrett, Auer, Mihalas, Hummer, Rybicki and many others, from 1965: application of computers to model non-LTE line formation numerically.

---

[1]An update of this finding is that the solar composition is the same as that of the oldest meteorites (carbonaceous chondrites) to very high precision, except for the five lightest elements and carbon. The earth has lost much of its hydrogen to space, while the sun has burned up 99% of its lithium — fortunately, not more than 6% of its hydrogen yet.

In these three exercises you will retrace some steps of the early pioneers. They don't require prior astronomy courses. The topics are:

- *spectral classification* (you in the role of Annie Cannon);

- *Saha-Boltzmann modeling of the Harvard classification* (you in the role of Cecilia Payne);

- *Schuster-Schwarzschild modeling of Fraunhofer line strengths* (you in the role of Marcel Minnaert).

The sequel sets of exercises *"Stellar Spectra B: LTE Line Formation"* and *"Stellar Spectra C: NLTE Line Formation"* treat more advanced spectral interpretation.
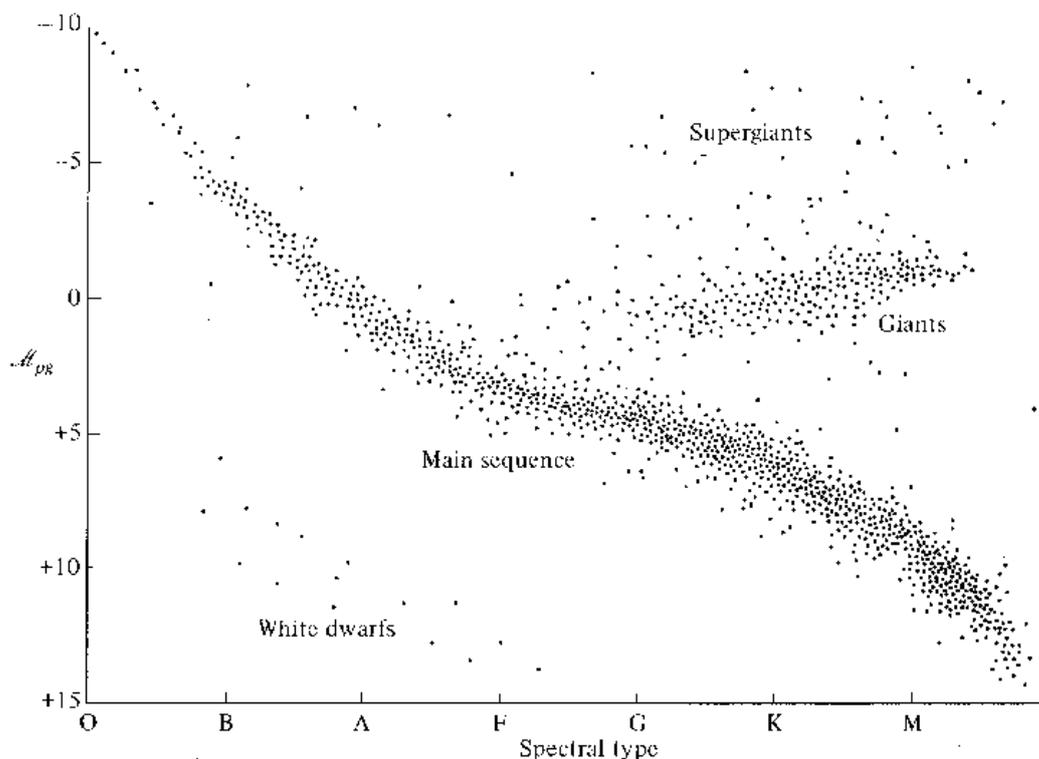

Figure 1: The Hertzsprung-Russell diagram (HRD). The Harvard spectral sequence along the x axis is the ordering as to spectral type that you will rediscover yourself in the first exercise. Stars to the right have red appearance, to the left they are blue. The photographically-determined absolute magnitude (luminosity at standard distance on a reversed logarithmic scale) is plotted along the y axis. Obviously the HRD is not filled at random but contains stars only in specific locations. Most stars lie on a diagonal band that is therefore called the "main sequence". Some other stars lie on a branch to the upper right called the "giant branch". Their presence implies that another parameter than only the spectral type is needed to define a star, the "luminosity classification" I–II–III–IV–V. Stars with luminosity class V are on the main sequence ("dwarfs") while stars with lower luminosity class (higher luminosity) are increasingly above it ("giants"). The point density in this HRD portrays stellar statistics: there are far more dwarfs than giants — but it is likely that many more white dwarfs exist than we observe. The stellar locations in the HRD correspond to the simple equation $L = 4\pi R^2 \, \sigma T_{\text{eff}}^4$ but when you are Annie Cannon in the first exercise you don't know that yet. You believe that spectral classification gauges important intrinsic stellar properties whatever they are — making it worthwhile to classify as many as as you can. From Novotny (1973).

1   Spectral classification ("Annie Cannon")

In this exercise you classify stellar spectra without prior knowledge — just as Annie Cannon did while setting up the Harvard sequence O – B – A – F – G – K – M.

Figure 2: Annie Jump Cannon (1863 – 1941) entered Harvard College Observatory in 1886 as an assistant to Edward Pickering, director of Harvard Observatory during 42 years. He was devoted to large-scale stellar spectrometry and set up the monumental "Henry Draper Catalague" of stellar spectra which was mostly assembled by Annie Cannon and her assistants, funded by a series of gifts from Mrs. Draper who wanted a memorial to her husband, the first spectroscopist to photograph a stellar spectrum (from a private observatory on the Hudson River). The effort started in 1886 (Draper died in 1882) and was concluded in 1924 with the publication of the 9th volume of the Catalogue in the Harvard Annals. By then, Mrs. Draper's quarter-million dollar bequest had yielded a quarter million stellar classifications. More history of astronomical spectroscopy is found in "The analysis of starlight" by Hearnshaw (1986), from which this photograph is copied.

1.1   Stellar spectra morphology

Figure 3 shows a set of photographic stellar spectrograms. They are rather like the spectrograms classified at Harvard. Note that they are negatives; stellar spectra usually contain absorption lines, dark on a brighter background (the "continuum").

- Cut the page into strips, one per spectrum, and order them into a morphological sequence. You are the first astronomer studying these spectra and you don't know what the coding is, except that the lines have something to do with the presence of specific elements.

- Try to explain all you see and speculate on the meaning of your ordering.

1.2   Data acquisition and spectral classification

This is a canned computer exercise for Windows from: `http://www.gettysburg.edu/academics/physics/clea/CLEAhome.html`.

- Get the CLEA-SPEC exercise (file `http://www.astro.uu.nl/~rutten/education/rjr-material/ssa/clea.zip`).

- Unzip `clea.zip` and install the CLEA-SPEC exercise.

- Start the exercise.

- Try out the various options. Classify a number of stellar spectra. Do the observing first if you prefer taking spectra before classifying them.

1.3 Introduction to IDL

We will use the interactive programming language IDL in the second and third exercise. The Student Edition suffices. First familiarize yourself with IDL. Under Windows it may be installed under Research Systems Inc. (RSI, an unfortunate acronym). Under Unix/Linux type `idl` in a terminal window, or `idlde` for a mouse-oriented environment.

- Start IDL.

- Work through the brief IDL manual at `http://www.astro.uu.nl/~rutten/education/rjr-material/idl/manuals`. You won't need the more advanced plotting and the input/output commands for these exercises.

- Write an IDL function `ADDUP(array)` as the one in the manual in a file `ADDUP.PRO` and try it out. You will need to put the file in a partition where you have write access, and to redirect IDL to that location (under Windows through `cd,'c:\yourdir\idl\'`).

1.4 Introduction to LaTeX

You should write a report in which you include the pertinent graphs made with IDL. You should explain everything seen in the graphs.

If you use LaTeX as text processor in order to gain experience in writing reports the astronomer's way then:

- Copy all files at `http://www.astro.uu.nl/~rutten/education/rjr-material/latex/student-report/` into your writing directory.

- Study file `latex-bibtex-manual.txt` and follow its instructions regarding file `report.tex`. The latter is a template for your report. Under Windows you may open it in WinEdt (`http://www.winedt.com/`) to process it with MikTex (`http://www.miktex.org/`). Under Unix or Linux insert it in a plain-text editor such as Emacs.

- Start writing, and frequently inspect the result.

- Experiment with PostScript or pdf figure insertion.

61 Cyg A

β Vir

Coma T60

HD 36936

16 Cyg A

γ Uma

HD 95735

HD 36865

78 Uma

HD 37129

Coma T 183

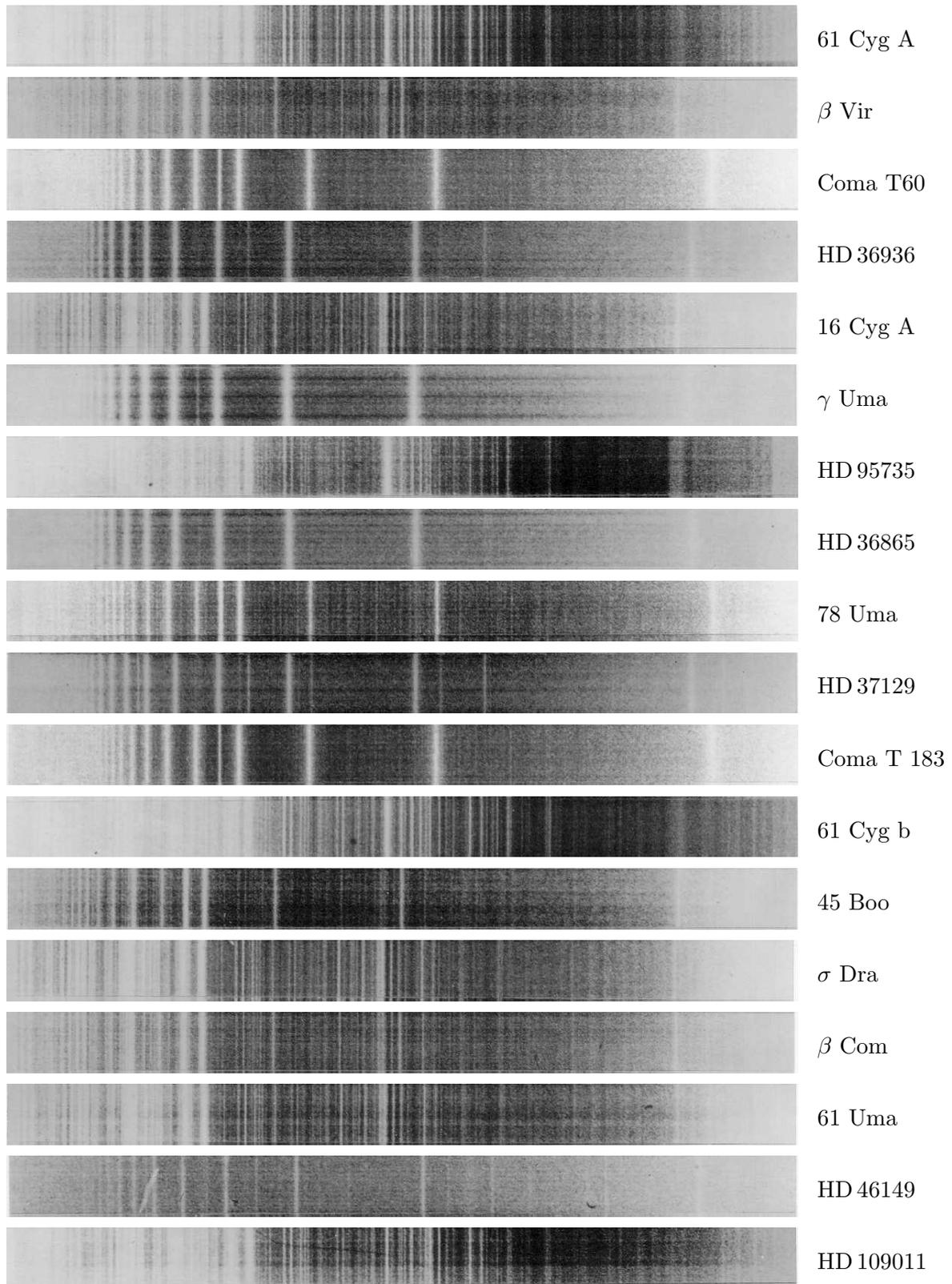61 Cyg b

45 Boo

σ Dra

β Com

61 Uma

HD 46149

HD 109011

Figure 3: Stellar spectrograms taken with a low-dispersion grating spectrometer. The wavelength increases to the right. From Abt et al. (1968).

5

2 Saha-Boltzmann calibration of the Harvard sequence ("Cecilia Payne")

In this exercise you will explain the spectral-type sequence that is studied morphologically in the first exercise and that is summarized in Figure 5. You so re-act the work of Cecilia Payne at Harvard. Her 1925 thesis was called "undoubtedly the most brilliant PhD thesis ever written in astronomy" by Otto Struve. Its opening sentences are:

> "The application of physics in the domain of astronomy constitutes a line of investigation that seems to possess almost unbounded possibilities. In the stars we examine matter in quantities and under conditions unattainable in the laboratory. The increase in scope is counterbalanced, however, by a serious limitation — the stars are not accessible to experiment, only to observation, and there is no very direct way to establish the validity of laws, deduced in the laboratory, when they are extrapolated to stellar conditions."

Extrapolation of terrestrial physics laws is precisely what Payne did in her thesis. She applied the newly derived Saha distribution for different ionization stages of an element to stellar spectra, finding that the empirical Harvard classification represents primarily a temperature scale. Her work crowned efforts of Saha, Russell, Fowler, Milne, Pannekoek and others along the same lines. It illustrates that detailed physics, in this case atomic physics, is usually needed to explain cosmic phenomena.

Figure 4: Cecilia Payne (1900 – 1979) was educated at Cambridge by Milne and Eddington. She went to the US in 1923 and spent the rest of her career at Harvard (Boston). Her 1925 thesis was the first one in astronomy at Harvard University and remains highly readable as a wide review of stellar spectroscopy at the time. The main conclusion was that stellar composition does not change much from star to star. Russell had already suggested so a decade earlier, but her thesis under Russells' guidance, published as the first Harvard Observatory Monograph, brought the point home. Copied from Hearnshaw (1986).

2.1 Payne's line strength diagram

The key graph in Payne's thesis (page 131, earlier published in Payne 1924) is reprinted in Figure 6. Clearly, the observed behavior in the upper panel is qualitatively explained by the computed behavior in the lower panel. We will recompute the latter.
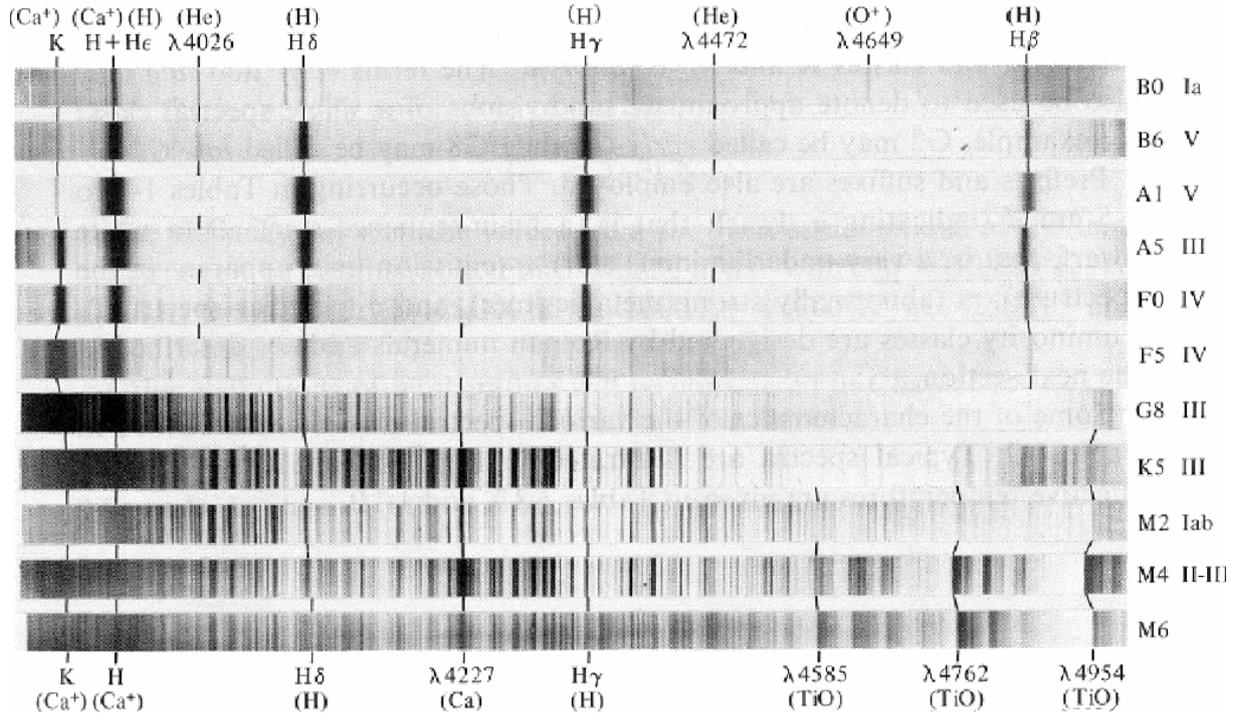
Figure 5: A selection of stellar spectrograms illustrating the Harvard spectral sequence. These example spectra are printed positively, with the absorption lines dark on a bright background. Wavelengths in Ångstrom (1 Å= 0.1 nm = 10^{-8} cm). The peak brightness shifts from left to right from the "early-type" stars (O and B) to the "late-type" stars (G and lower). The sun has spectral type G2 V and is a late-type star. The early-type stars display the hydrogen Balmer lines prominently, but these become weak in solar-type spectra in which the Ca^+ H and K resonance lines are strongest. The M dwarfs on the bottom display strong molecular bands. From Novotny (1973).

2.2 The Boltzmann and Saha laws

In thermodynamical equilibrium (TE) macroscopic equipartition laws hold with the gas temperature as the major parameter. These are the Kirchhoff, Planck, Wien and Stefan-Boltzmann laws for radiation, and the Maxwell, Saha and Boltzmann laws for matter. In this exercise we are concerned with the latter two. They describe the division of the particles of a specific element over its different ionization stages and over the discrete energy levels within each stage. For example, the Saha law specifies the distribution of iron particles between neutral iron (Fe), once-ionized iron (Fe^+), twice-ionized iron (Fe^{2+}), etc., whereas the Boltzmann law specifies the sub-distribution of the iron particles per ionization stage over the discrete energy levels that each of the Fe, Fe^+, Fe^{2+} etc.[2] stages may occupy. Figure 7 illustrates the energy level structure of neutral hydrogen.

Boltzmann law. In TE the partitioning of a specific atom or ion stage over its discrete energy levels ("excitation equilibrium") is given by the *Boltzmann distribution*

$$\frac{n_{r,s}}{N_r} = \frac{g_{r,s}}{U_r}\, \mathrm{e}^{-\chi_{r,s}/kT}, \tag{1}$$

---

[2]In astronomy one doesn't write ions as Fe^{3+} but rather as Fe IV. More precisely: Fe I is the *spectrum* of neutral iron Fe, Fe II the *spectrum* of once-ionized iron Fe^+, etc.
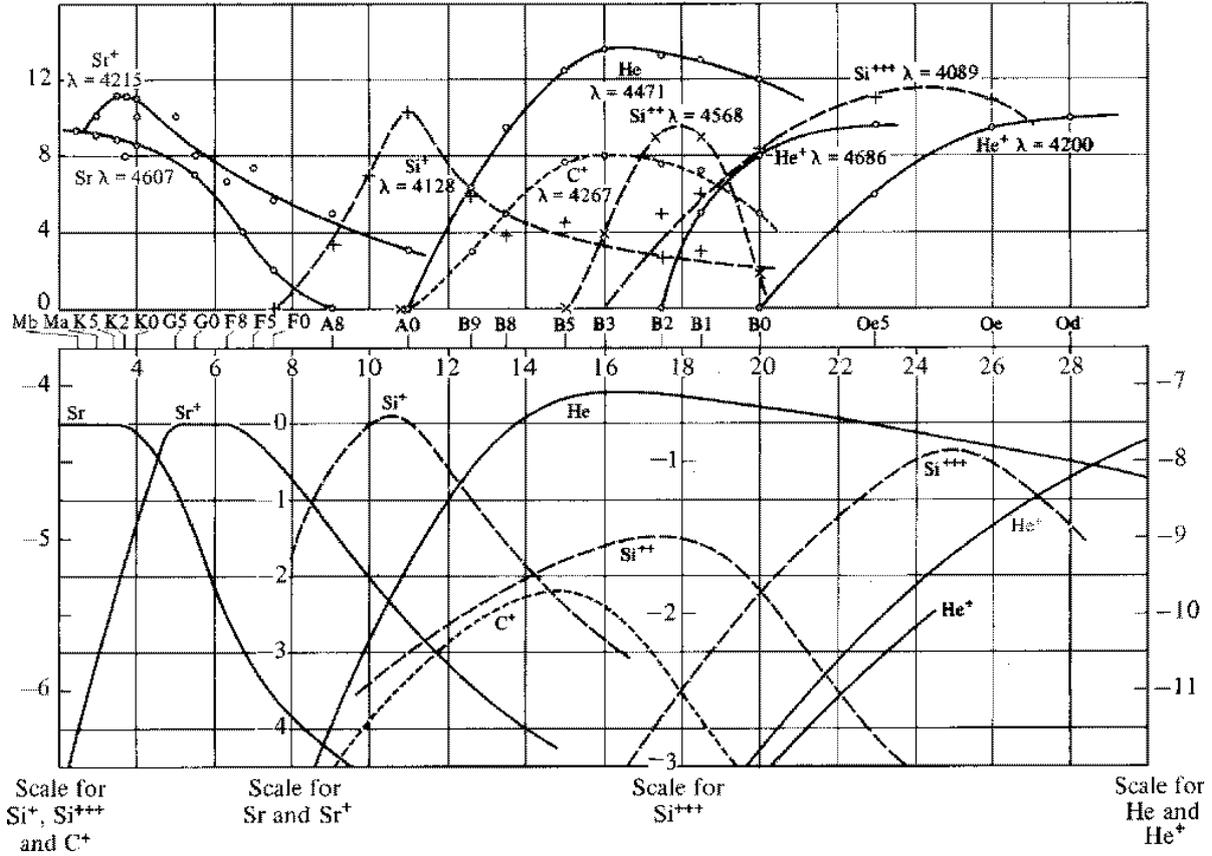
Figure 6: The strengths of selected lines along the spectral sequence. Upper panel: variations of observed line strengths with spectral type in the Harvard sequence. The latter is plotted in reversed order on a non-linear scale that was obtained by making the peaks coincide with the corresponding peaks in the lower panel. The y-axis units are eye estimates on an arbitrary scale. Lower panel: Saha-Boltzmann predictions of the fractional concentration $N_{r,s}/N$ of the lower level of the lines indicated in the upper panel, each labeled with its ionization stage, on logarithmic y-axis scales that are specified per species at the bottom, against temperature T along the x axis given in units of 1000 K along the top. The pressure was taken constant at $P_e = N_e kT = 131$ dyne cm$^{-2} = 13.1$ Pascal. From Novotny (1973) who took it from Payne (1924).

with T the temperature, k the Boltzmann constant, $n_{r,s}$ the number of particles per cm^3 in level s of ionization stage r, $g_{r,s}$ the statistical weight of that level, and $\chi_{r,s}$ the excitation energy of that level measured from the ground state $(r, 1)$, $N_r \equiv \sum_s n_{r,s}$ the total particle density in all levels of ionization stage r, and U_r its *partition function*[3] defined by

$$U_r \equiv \sum_s g_{r,s}\, \mathrm{e}^{-\chi_{r,s}/kT}. \tag{2}$$

Thus, the neutral stage has $r = 1$, each ground state is at $s = 1$, and each ground state has excitation energy $\chi_{r,1} = 0$. and ionization energy to the next stage χ_r. A radiative deexcitation between levels (r, s) and (r, t), with level s "higher" than level t, releases a photon with energy $\chi_{r,s} - \chi_{r,t} = h\nu = hc/\lambda$, with h the Planck constant, ν the photon frequency, c the velocity of light and λ the wavelength. The excitation energy $\chi_{r,s}$ is the energy difference between the excited level (r, s) and the ground state $(r, 1)$. Astronomers usually call it "excitation
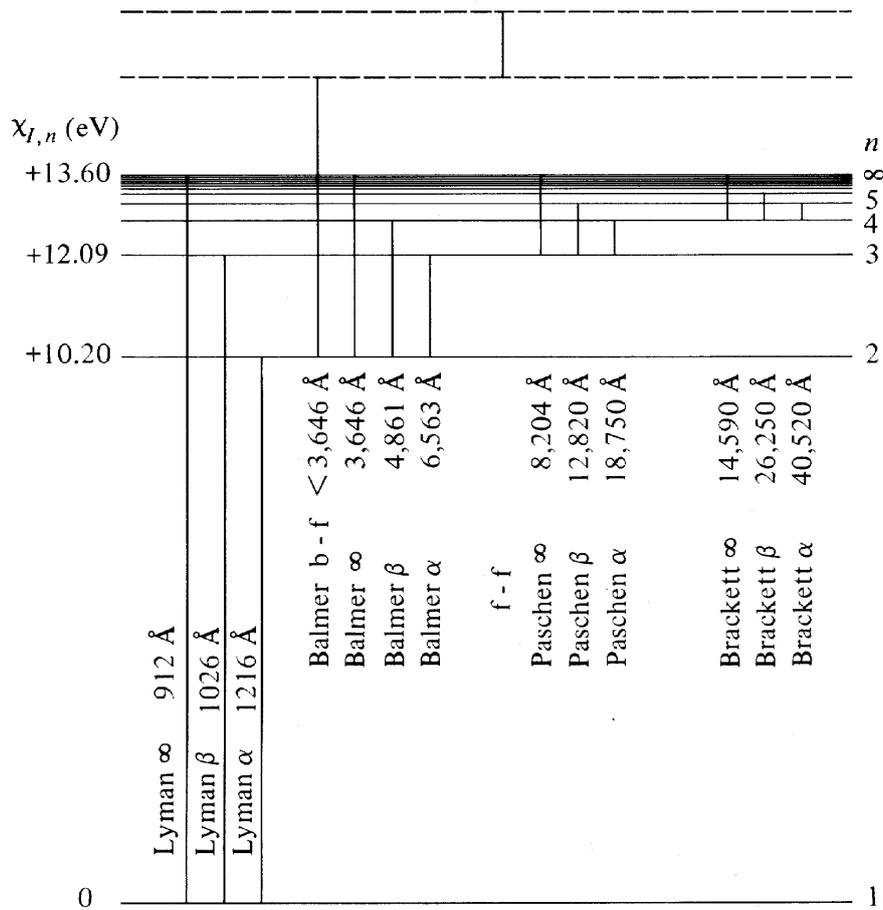
---

[3]Dutch: toestandssom.

Figure 7: Energy level diagram for hydrogen. The bound levels are at excitation energies given by (5) on page 19. They approach the ionization threshold at $\chi_H = 13.598$ eV for $n \to \infty$. The principal quantum number n equals the level counter s in this simple structure. The fine structure of each level (splitting in $2n^2$ sublevels) is not shown. For each of the first four hydrogen series the principal bound-bound transitions between bound levels are marked by vertical lines with the name and the wavelength of the corresponding spectral line. The series limits ($n = \infty$) are also marked. A bound-free ioniza-tion/recombination transition is added to the Balmer series. The amount of energy above the ionization threshold represents the kinetic energy that is gained or lost. A free-free transition (radiative encounter between a bare proton and a free electron) is also marked. The bound-free and free-free transitions con-tribute to stellar continua, while the bound-bound transitions produce the hydrogen lines. The Lyman lines are in the ultraviolet, the Balmer lines are in the visible and the Paschen and Brackett lines are in the infrared. Some Balmer lines are present in the stellar spectrograms in Figure 5. The solar Balmer α line (usually called Hα) is shown in Figure 9. From Novotny (1973).

potential" and measure it from the ground state up[4] in electron volt, with 1 eV corresponding to 1.6022×10^{-12} erg (1.6022×10^{-19} Joule). For example, the H I Balmer α line results from photonic transitions between levels $n = 2$ and $n = 3$ of neutral hydrogen, with $\chi_{1,3} = 12.09$ eV, $\chi_{1,2} = 10.20$ eV and wavelength $\lambda = hc/(\chi_{1,3} - \chi_{1,2}) = 656.3$ nm (Figure 7).

The number densities $n_{r,s}$ and $n_{r,t}$ are called "level populations" and are usually measured per

---

[4]Physicists often measure level energies as "binding energy" from the ground state of the next ion down in wavenumbers (cm^{-1}).
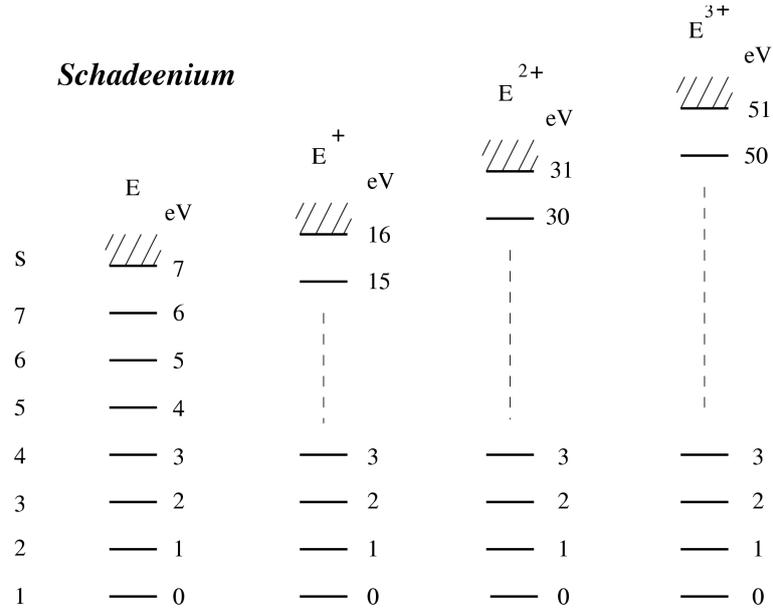
Figure 8: *Energy level diagram for Schadee's element E, showing the neutral stage (lefthand column, $r = 1$) and the first three ionization stages ($r = 2 - 4$). The level energies increase in 1 eV steps. The columns may be thought of as being stacked on top of each other since each ion requires the previous stage to be ionized. The level counter s starts at 1 within each stage (but IDL starts at 0, as do the level energies). In astronomical convention the spectra of neutral schadeenium E, ionized schadeenium E^+ and doubly ionized schadeenium E^{2+} are called EI, EII, and EIII, respectively.*

cm^3.

The statistical weights $g_{r,s}$ measure the degeneracy of levels due to magnetic fine splitting. The latter occurs only in the presence of an external magnetic field; in its absence, magnetic fine-structure levels coincide and may accommodate more particles than allocated per single level by the Pauli exclusion principle. The weights measure such excess. For example, neutral hydrogen atoms have $g_{1,1} = 2$ for their ground state because the electron and proton spins can be parallel or anti-parallel[5].

- Inspect the hydrogen energy level diagram in Figure 7. Which transitions correspond to the hydrogen lines in Figure 5? Which transitions share lower levels and which share upper levels?

- Payne's basic assumption was that the strength of the absorption lines observed in stellar spectra increases with the population density of the lower level of the corresponding transition. Why might this be a reasonable assumption (it is)?

- Use this expectation to give initial rough estimates of the strength ratios of the α lines in the the HI Lyman, Balmer, Paschen and Brackett series.

---

[5]The fine-structure transition between the two states produces the 21 cm radio line from interstellar gas.

Saha law. In TE the particle partitioning over the various ionization stages of an element ("ionization equilibrium") is given by the *Saha distribution*:

$$\frac{N_{r+1}}{N_r} = \frac{1}{N_{\mathrm{e}}} \frac{2U_{r+1}}{U_r} \left(\frac{2\pi m_{\mathrm{e}} kT}{h^2}\right)^{3/2} \mathrm{e}^{-\chi_r/kT}, \tag{3}$$

with N_{e} the electron density, m_{e} the electron mass, χ_r the threshold energy needed to ionize stage r to stage $r+1$, and U_{r+1} and U_r the partition functions of ionization stages $r+1$ and r defined by (2). The ionization energy χ_r is the minimum photon energy that is absorbed at ionization or emitted at recombination in a bound-free interaction. The factor two represents the statistical weight of the freed electron, which has $g_{\mathrm{e}} = 2$ due to the two orientations that its spin may take. The scaling with $1/N_{\mathrm{e}}$ says that ionization is easier if there is room for the resulting free electron or, reversedly, that recombination from stage $r+1$ to stage r requires catching a free electron. The kinetic energy of the free electron contributes the $(\ldots)^{3/2}$ term through the Maxwell velocity distribution.

U_r	5 000 K	10 000 K	20 000 K
U_1	1.11	1.46	2.23
$U_2 = U_3 = U_4$	1.11	1.46	2.27

$n_{r,s}/N_r$	5 000 K	10 000 K	20 000 K
s = 1	0.90	0.69	0.45–0.44
2	0.09	0.22	0.25
3	0.01	0.07	0.14
4	(-3)	0.02	0.08
5	(-4)	0.01	0.04
6	(-5)	(-3)	0.02
7	(-6)	(-3)	0.01
10	[(-10)]	(-5)	(-3)
15	[(-15)]	(-8)	(-4)

N_r/N	ion	5 000 K	10 000 K	20 000 K
r = 1	E	0.91	(-4)	(-10)
2	E^+	0.09	0.95	(-4)
3	E^{2+}	(-11)	0.05	0.63
4	E^{3+}	(-36)	(-11)	0.37
5	E^{4+}	(-82)	(-29)	(-6)

Table 1: Schadee's Saha-Boltzmann population tables for element E. The quantity $N = \sum N_r$ is the total density per cm^3 of particles of element E. The notation (-i) stands for order of magnitude $\approx 10^{-i}$. The bracketed values in the 5 000 K column of the second table are for levels that do not exist in the neutral stage E.

2.3 Schadee's tables for schadeenium

This section gives Saha-Boltzmann results for a hypothetical (but iron-like) element in conditions similar to a stellar atmosphere. They are taken from old lecture notes by Schadee[6]. He called

---

[6]Aert Schadee (1936 – 1999) was a solar physicist at Utrecht University. He started under Minnaert's guidance as a spectroscopist concentrating on solar molecular line formation (Schadee 1964), then developed the theory

his element "E" but I call it "schadeenium" now. It has:

- ionization energies $\chi_1 = 7$ eV for neutral E, $\chi_2 = 16$ eV for E$^+$, $\chi_3 = 31$ eV for E^{2+}, $\chi_4 = 51$ eV for E^{3+};
- excitation energies that increase incrementally by 1 eV: $\chi_{r,s} \equiv s - 1$ eV in each stage;
- statistical weights $g_{r,s} \equiv 1$ for all levels (r, s).

Schadee evaluated the Saha and Boltzmann laws for element E, electron pressure $P_e = N_e\,k\,T = 10^3$ dyne cm^{-2} and temperature $T = 5\,000, 10\,000$ and $20\,000$ K, respectively. The corresponding distributions specified by (1)–(3) are given in Schadee's tables in Table 1.

- Note in the first table that the partition functions computed from (2) are of order unity and barely sensitive to temperature.

- In the second table, note the steep Boltzmann population decay with $\chi_{r,s}$ given by (1). It is less steep for higher temperature. The columns add up to unity because the values in this table are scaled by N_r. They therefore depend on U_r, but the small variation between U_1 and U_4 in the first table produces a difference at two-digit significance only for $s = 1$ at $20\,000$ K. The partition function U_1 of the neutral stage is the sum of only seven levels; the higher levels present in stages $r \geq 2$ contribute only marginally. The ground state always has the largest population.

Thus, the lowest levels are the most important ones, due to the rapid decay of the Boltzmann factor $e^{-\chi/kT}$ with $\chi_{r,s}$. This explains the insensitivity of U_r to temperature in the first table. Real atoms and ions tend to have larger energy difference between levels 1 and 2, so that their partition function is often well approximated by the statistical weight of the ground state.

- Inspect the third table, computed from (3). There are only two ionization stages significantly present per column. For $T = 5\,000$ K element E is predominantly neutral, for $T = 10\,000$ K it is once ionized (E$^+$), for higher temperature stages E^{2+} and E^{3+} appear while E and E$^+$ vanish.

There is a striking difference between the Boltzmann and the Saha dependencies on temperature. Ionization may fully deplete the ground stage (third table), whereas excitation never depletes the ground state by itself (second table) but only changes the steepness of the exponential decay.

- Explain from (1) and (3) why the Saha and Boltzmann distributions behave differently for increasing temperature.

- Speculate why ionization can fully deplete a stage even though excitation puts only a few atoms in levels below the ionization level. Hint: what parameter in the Saha distribution can cause equality between high-level and next-ion population at a given temperature?

Summary: in TE one expects to find only at most two adjacent ionization stages to be present in a gas of given temperature, with more or less steep exponential population decay with excitation energy within each ionization stage.

$$\boxed{\begin{aligned}
&\text{1 \AA} = 0.1 \text{ nm} = 10^{-8} \text{ cm} \\
&\text{1 erg} = 10^{-7} \text{ Joule} \\
&\text{1 dyne cm}^{-2} = 0.1 \text{ Pascal} = 10^{-6} \text{ bar} = 9.8693 \times 10^{-7} \text{ atmosphere} \\
&\text{energy of 1 eV} = 1.60219 \times 10^{-12} \text{ erg} \\
&\text{photon energy (in eV) } E = 12398.55/\lambda \text{ (in \AA)} \\
&\text{speed of light } c = 2.99792 \times 10^{10} \text{ cm s}^{-1} \\
&\text{Planck constant } h = 6.62607 \times 10^{-27} \text{ erg s} \\
&\text{Boltzmann constant } k = 1.38065 \times 10^{-16} \text{ erg K}^{-1} \\
&\qquad\qquad\qquad\qquad\quad = 8.61734 \times 10^{-5} \text{ eV K}^{-1} \\
&\text{electron mass } m_{\text{e}} = 9.10939 \times 10^{-28} \text{ g} \\
&\text{proton mass } m_{\text{p}} = 1.67262 \times 10^{-24} \text{ g} \\
&\text{atomic mass unit (amu, C=12) } m_{\text{A}} = 1.66054 \times 10^{-24} \text{ g} \\
&\text{first Bohr orbit radius } a_0 = 0.529178 \times 10^{-9} \text{ cm} \\
&\text{hydrogen ionization energy } \chi_{\text{H}} = 13.598 \text{ eV}
\end{aligned}}$$

Table 2: Selected units and constants. Precise values available at http://physics.nist.gov/cuu/Constants.

2.4   Saha-Boltzmann populations of schadeenium

We will now reproduce Schadee's tables by writing IDL routines that compute U_r from (2), $n_{r,s}/N_r$ from (1), and N_r/N from (3) for element E. Table 2 specifies various units and constants (using cgs units in order to expose you to the real world — as seen by astronomers).

- Start a file `SSA2.PRO` to develop this exercise as an IDL main program. It should get the form:

```
function something, inputparameter, inputparameter
  IDL statement
  IDL statement
  return, outputparameter
end

pro something, inputparameter, inputparameter
  IDL statement
  IDL statement
end



IDL statement    ; comment
IDL statement    ; comment
STOP             ; comment out or delete when fine

IDL statement
IDL statement


end
```

14

The IDL routines (functions and procedures) come at the top of this file or in separate `NAME.PRO` files. Start with plain IDL statements in `SSA2.PRO` and convert these into a routine when you are happy with them. Process the file to try out your command sequences by saving it and typing `.run ssa2.pro` on the IDL command line.

Adding `STOP` statements to the file makes IDL stop right there, so that you can inspect intermediate results on the command line. Typing `help,parameter` lets you inspect your parameter types. Typing `print,parameter` displays the current parameter value. You can also type individual IDL statements on the command line one by one to try them out. The up cursor arrow brings back previous commands so that you don't have to retype them. IDL continues the program when you type `.con` (or just `.c`; IDL accepts non-ambiguous abbreviations). Typing a question mark starts up the IDL help utility.

- Compute the partition functions U_r of the Schadee element:

```
u=fltarr(4)                ; declare 4-element float array; set values 0
chiion=[7,16,31,51]        ; Schadee ionization energies into integer array
k=8.61734D-5               ; Boltzmann constant in eV/deg (double precision)
temp=5000.                 ; the decimal point makes it a float
for r = 0,3 do $           ; a $ sign extends a command to the next line
  for s = 0, chiion(r)-1 do u(r)=u(r) + exp(-s/(k*temp))
print,u                    ; print resulting values for U(0)...U(3)
```

Note that IDL starts counting at zero (just as the eV scale for the levels of element E). The double precision of the Boltzmann constant forces double precision for the evaluation of the exponential which gets very small for large s. (If a result exceeds the IDL numerical word length IDL issues a warning, but it will not break off processing.)

- Compare your results for `temp=5000`, `temp=10000` and `temp=20000` to Schadee's first table on page 12.

- Now turn the above into a function "`PARTFUNC_E,temp`" for future use:

```
function partfunc_E, temp
  ; partition functions Schadee element
  ; input: temp (K)
  ; output: fltarr(4) = partition functions U1,..,U4
u=fltarr(4)
chiion=[7,16,31,51]
k=8.61734D-5
for r = 0,3 do $
  for s = 0, chiion(r)-1 do u(r)=u(r) + exp(-s/(k*temp))
return,u
end
```

It has to go to the top of your `SSA2.PRO` file or to an independent `PARTFUNC_E.PRO` file and it should produce:

```
IDL> .r ssa2.pro                         ; .r suffices for .run
% Compiled module: PARTFUNC_E.
IDL> print,partfunc_E(5000)
      1.10887      1.10888      1.10888      1.10888
IDL> print,partfunc_E(10000)
      1.45590      1.45634      1.45634      1.45634
IDL> print,partfunc_E(20000)
      2.23243      2.27134      2.27155      2.27155
```

- Then write a Boltzmann routine which computes $n_{r,s}/N_r$ from (1):

```
function boltz_E,temp,r,s
 ; compute Boltzmann population for level r,s of Schadee element E
 ; input: temp (temperature, K)
 ;         r (ionization stage nr, 1 - 4 where 1 = neutral E)
 ;         s (level nr, starting at s=1)
 ; output: relative level population n_(r,s)/N_r
u=partfunc_E(temp)
keV=8.61734D-5        ; Boltzmann constant in ev/deg
relnrs = 1./u(r-1)*exp(-(s-1)/(keV*temp))
return, relnrs
end
```

- Check its working by reproducing the second Schadee table on page 12 for the three temperatures:

```
IDL> for s=1,10 do print,boltz_E(5000,1,s)
       0.90181500
       0.088544707
      0.0086937622
      0.00085359705
      8.3810428e-05
      8.2289270e-06
      8.0795721e-07
      7.9329280e-08
      7.7889454e-09
      7.6475762e-10
```

- Then write a Saha routine to reproduce Schadee's third table on page 12. It gives N_r/N where $N = \sum N_r$ is the total element density. The simplest way to get this ratio is to set N_1 to some value, evaluate the four next full-stage populations successively from (3), and divide them by their sum $= N$ in the same scale:

```
function saha_E,temp,elpress,ionstage
 ; compute Saha population fraction N_r/N for Schadee element E
 ; input: temperature, electron pressure, ion stage
; physics constants
kerg=1.380658D-16          ; Boltzmann constant (erg K; double precision)
kev=8.61734D-5             ; Boltzmann constant (eV/deg)
h=6.62607D-27              ; Planck constant (erg s)
elmass=9.109390D-28        ; electron mass (g)
```

```
; kT and electron density
kevT=kev*temp
kergT=kerg*temp
eldens=elpress/kergT
chiion=[7,16,31,51]        ; ionization energies for element E
u=partfunc_E(temp)         ; get partition functions U(0)...u(3)
u=[u,2]                    ; add estimated fifth value to get N_4 too
sahaconst=(2*!pi*elmass*kergT/(h*h))^1.5 * 2./eldens
nstage=dblarr(5)           ; double-precision float array
nstage(0)=1.               ; relative fractions only (no abundance)
for r=0,3 do $
   nstage(r+1) = nstage(r)*sahaconst*u(r+1)/u(r)*exp(-chiion(r)/kevT)
ntotal=total(nstage)       ; sum all stages = element density
nstagerel=nstage/ntotal    ; fractions of element density
return,nstagerel(ionstage-1)
end
```

The double precision declarations again avoid error messages from too small exponentials.

- The IDL **TOTAL(array)** function used above sums the elements of an arry of any dimension. Check it out in the Online Help (?).

- Check your Saha routine against Schadee's third table on page 12:

```
IDL> for r=1,5 do print,saha_E(20000,1e3,r)
   2.7277515e-10
   0.00018027848
       0.63200536
       0.36781264
   1.7197524e-06
IDL> for r=1,5 do print,saha_E(20000,1e1,r)
   7.2875161e-16
   4.8163564e-08
     0.016884783
     0.98265572
   0.00045945253
```

The second example shows the larger degree of ionization that occurs at lower pressure.

2.5 Payne curves for schadeenium

If TE holds in a stellar atmosphere one may expect that the observed strength of a spectral line involving level (r, s) scales with the Saha-Boltzmann prediction for the lower level population $n_{r,s}$ — even if one doesn't know how spectral lines are formed in detail. That was the underlying premise of Payne's analysis. We follow it by plotting curves as in the lower panel of Figure 6 for various levels of the neutral and ionization stages of element E.

- Write a function "**SAHABOLT_E,temp,elpress,r,s**" that evaluates $n_{r,s}/N$ for any level of E as a function of T and P_e:

```
        function sahabolt_E,temp,elpress,ion,level
          ; compute Saha-Boltzmann populaton n_(r,s)/N for level r,s of E
          ; input: temperature, electron pressure, ionization stage, level nr
        return, saha_E(temp,elpress,ion) * boltz_E(temp,ion,level)
        end
```

- Inspect a few values:

```
        IDL> for s=1,5 do print,sahabolt_E(5000,1e3,1,s)
               0.81709346
              0.080226322
             0.0078770216
             0.00077340538
             7.5936808e-05
        IDL> for s=1,5 do print,sahabolt_E(20000,1e3,1,s)
             1.2218751e-10
             6.8397163e-11
             3.8286827e-11
             2.1431900e-11
             1.1996980e-11
        IDL> for s=1,5 do print,sahabolt_E(10000,1e3,2,s)
               0.64895420
               0.20334646
              0.063717569
              0.019965573
             0.0062561096
        IDL> for s=1,5 do print,sahabolt_E(20000,1e3,4,s)
              0.16192141
              0.090639095
              0.050737241
              0.028401295
              0.015898254
```

These values represent multiplications of Schadee's second and third tables. They illustrate
again that within a single ionization stage the lower levels always have higher population due
to the Boltzmann factor. The drop-off with s is less steep at higher temperature. The overall
population per stage is set by the Saha law.

- Compute the ground-state populations $n_{r,1}/N$ for Payne's pressure ($P_e = 131$ dyne cm^{-2})
and a range of temperatures for each ion r, and plot them together in a Payne-like graph:

```
        temp=1000*indgen(31)        ; make array 0,...,30000 in steps of 1000 K
        print,temp                  ; check
        pop=fltarr(5,31)            ; declare float array for n(r,T)
        for T=1,30 do $             ; $ continues statement to next line
          for r=1,4 do pop(r,T)=sahabolt_E(temp(T),131.,r,1)
        plot,temp,pop(1,*),/ylog,yrange=[1E-3,1.1], $
            xtitle='temperature',ytitle='population'
        oplot,temp,pop(2,*)         ; first ion stage in the same graph
        oplot,temp,pop(3,*)         ; second ion stage
        oplot,temp,pop(4,*)         ; third ion stage
```

- What causes the steep flanks on the left and the right side of each peak? What happens for $T \downarrow 0$ and for $T \uparrow \infty$?

- Payne plotted her curves for the actual lower levels of the lines specified by their wavelengths in the upper panel, including their Boltzmann factor. Study its influence on your E curves by adding curves for higher values of s to your plot:

  ```
  for T=1,30 do $                 ; repeat for s=2 (excitation energy = 1 eV)
    for r=1,4 do pop(r,T)=sahabolt_E(temp(T),131.,r,2)
  oplot,temp,pop(1,*)
  oplot,temp,pop(2,*)
  oplot,temp,pop(3,*)
  oplot,temp,pop(4,*)
  for T=1,30 do $                 ; repeat for s=4 (excitation energy = 3 eV)
    for r=1,4 do pop(r,T)=sahabolt_E(temp(T),131.,r,4)
  oplot,temp,pop(1,*)
  oplot,temp,pop(2,*)
  oplot,temp,pop(3,*)
  oplot,temp,pop(4,*)
  ```

- Explain the changes between the three sets of curves. What happens for elements with lower/higher ionization energies than E has?

2.6   Discussion

The E curves in your plot indeed resemble Payne's curves in Figure 6. In order to reproduce her lower panel in detail you would have to evaluate the partition functions for the actual elements that she used and to enter the actual excitation energies of the lower levels of the lines that she used. More work, but in principle not different from what you have done for element E. So, you have confirmed Payne's conclusion that the Harvard classification of stellar spectra is primarily an ordering with temperature, controlled by Saha-Boltzmann population statistics. In following her footsteps, you have crossed the border between morphological description and physical modeling, from astronomy to astrophysics. Congratulations!

2.7   Saha-Boltzmann populations of hydrogen

It is easy to write an exact Saha-Boltzmann routine for hydrogen. Its ionization energy $\chi_1 = 13.598$ eV; the statistical weights $g_{r,s}$ and level energies $\chi_{r,s}$ of neutral hydogen are given by

$$g_{1,s} = 2\,s^2 \tag{4}$$
$$\chi_{1,s} = 13.598\,(1 - 1/s^2) \quad \text{eV} \tag{5}$$

while the single ion stage (bare protons) has $U_2 = g_{2,1} = 1$.

- Write a function "SAHABOLT_H,temp,elpress,s" that produces the population of hydrogen level s (of course by copying bits and pieces with cut & paste from your routines for element E):

  ```
  function sahabolt_H,temp,elpress,level
    ; compute Saha-Boltzmann population n_(1,s)/N_H for hydrogen level
    ; input: temperature, electron pressure, level number
  ```

19

```
; physics constants
kerg=1.380658D-16          ; Boltzmann constant (erg K; double precision)
kev=8.61734D-5             ; Boltzmann constant (eV/deg)
h=6.62607D-27              ; Planck constant (erg s)
elmass=9.109390D-28        ; electron mass (g)
; kT and electron density
kevT=kev*temp
kergT=kerg*temp
eldens=elpress/kergT
; energy levels and weights for hydrogen
nrlevels=100                    ; reasonable partition function cut-off value
g=intarr(2,nrlevels)            ; declaration weights (too many for proton)
chiexc=fltarr(2,nrlevels)       ; declaration excitation energies (idem)
for s=0,nrlevels-1 do begin     ; enclose multiple lines with begin...end
  g(0,s)=2*(s+1)^2                    ; statistical weights
  chiexc(0,s)=13.598*(1-1./(s+1)^2)    ; excitation energies
endfor                          ; begin...end cannot go on command line!
g(1,0)=1                        ; statistical weight free proton
chiexc(1,0)=0.                  ; excitation energy proton ground state
; partition functions
u=fltarr(2)
u(0)=0
for s=0,nrlevels-1 do u(0)=u(0)+ g(0,s)*exp(-chiexc(0,s)/kevT)
u(1)=g(1,0)
; Saha
sahaconst=(2*!pi*elmass*kergT/(h*h))^1.5 * 2./eldens
nstage=dblarr(2)                ; double-precision float array
nstage(0)=1.                    ; relative fractions only
nstage(1) = nstage(0) * sahaconst * u(1)/u(0) * exp(-13.598/kevT)
ntotal=total(nstage)            ; sum both stages = total hydrogen density
; Boltzmann
nlevel = nstage(0)*g(0,level-1)/u(0)*exp(-chiexc(0,level-1)/kevT)
nlevelrel=nlevel/ntotal         ; fraction of total hydrogen density
;stop                           ; in for parameter inspection
return,nlevelrel
end
```

- Computing the exact partition function this way is a bit overdone since it turns out that $U(1)$ $(= \mathtt{u(0)}) = g_{1,1} = 2.00000$. You can see this by activating the STOP statement before the RETURN statement and then listing internal subroutine parameters:

```
IDL> .r ssa2.pro
IDL> print,sahabolt_H(5000,1e2,1)
% Stop encountered:  SAHABOLT_H        115 ssa2.pro
IDL> print,u
      2.00000        1.00000
```

```
IDL> for s=0,5 do print,s+1,g(0,s),chiexc(0,s),$
IDL>   g(0,s)*exp(-chiexc(0,s)/kevT)
       1        2     0.00000       2.0000000
       2        8     10.1985   4.2020652e-10
       3       18     12.0871   1.1803501e-11
       4       32     12.7481   4.5249678e-12
       5       50     13.0541   3.4757435e-12
       6       72     13.2203   3.4032226e-12
IDL> for s=0,nrlevels-1,10 do print,s+1,g(0,s),chiexc(0,s),$
IDL>   g(0,s)*exp(-chiexc(0,s)/kevT)
       1        2     0.00000       2.0000000
      11      242     13.4856   6.1790222e-12
      21      882     13.5672   1.8637147e-11
      31     1922     13.5838   3.9070233e-11
      41     3362     13.5899   6.7387837e-11
      51     5202     13.5928   1.0357868e-10
      61     7442     13.5943   1.4763986e-10
      71    10082     13.5953   1.9957013e-10
      81    13122     13.5959   2.5936970e-10
      91    16562     13.5964   3.2703819e-10
```

The excitation energies were already illustrated in Figure 7 on page 10. The first excited level $s = 2$ is at such high excitation energy that its small Boltzmann factor makes its population negligible in comparison with the ground state population. However, the increase with s at large values of s shows that the hydrogen partition function would get infinite if too many levels are included in the summation, because $g_{1,s} \sim s^2$ while $\chi_{1,s} \to 13.598$. Actually, all atoms and ions share in this behavior at very high excitation energy since they all get to be "hydrogenic" in nature when the valence electron sits in a nearly detached orbit. This singularity has been a cause of much debate, but real atoms are not worried by it. They are never alone[7] and loose their identity through interactions with neighbours long before they grow as large as this. A reasonable cut-off value to the orbit size is set by the mean atomic interdistance $N^{-1/3}$ (page 260 of Rybicki and Lightman 1979):

$$s_{\mathrm{max}} \approx \sqrt{\frac{r}{a_0}} \ N^{-1/6}, \tag{6}$$

giving $s_{\mathrm{max}} \approx 100$ for hydrogen at $N_{\mathrm{H}} = 10^{12}$ cm^{-3}. With such a cut-off the partition functions are generally not much larger than the ground state weights at all temperatures of interest — those at which the pertinent stage of ionization is not devoid of population anyhow.

2.8   Solar Ca$^+$ K versus Hα: line strength

Figure 5 on page 8 shows that in solar-type stars the hydrogen Balmer lines become much weaker than the Ca$^+$ K $s = 2 - 1$ line at $\lambda = 3933.7$ Å (called the calcium K line[8]). The spectrograms in Figure 5 do not include the principal line of the Balmer sequence, the hydrogen

---

[7]They are never alone where TE holds. In intergalactic space they may be quite lonely, but they won't sit in their high levels out there.

[8]The astronomical notation is Ca II K. The K is an extension from Draper to the original alphabetic solar spectrum feature list by Fraunhofer, who only named Ca II H.

$s = 3 - 2$ line at $\lambda = 6563$ Å which is called the Hα line (see the hydrogen term diagram in Figure 7 on page 10), but even this line gets much weaker than Ca$^+$ K in solar-type stars. This is demonstrated in Figure 9 which shows high-precision tracings of the solar spectrum around these two wavelengths. Obviously, the main line in the lefthand panel (Ca$^+$ K) is much stronger than the one at right (Hα). Since stars as the sun are mostly made up of hydrogen, it may come as a surprise that a calcium line is much stronger than a hydrogen line. However, by now (in your role of being Cecilia Payne) it is clear to you that line strength ratios between different elements do not only depend on their abundance ratio but also on the temperature. We will quantify this dependence for this solar line pair.
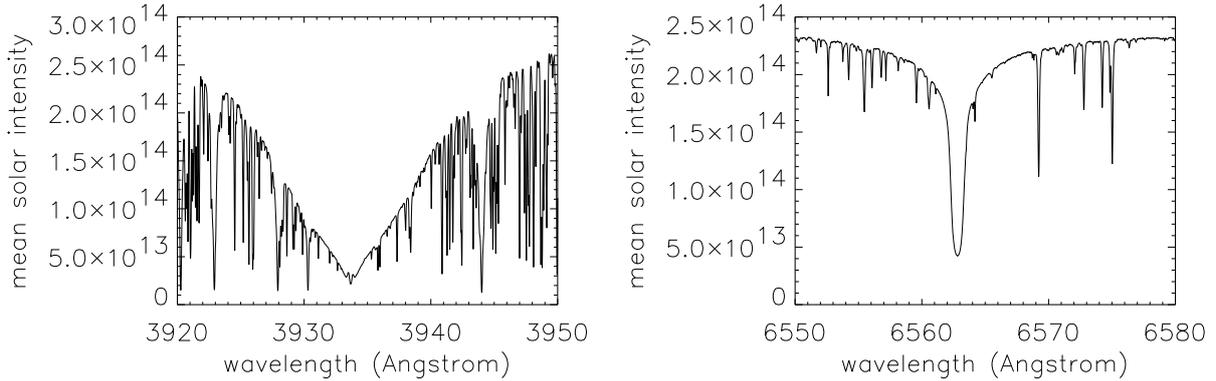

Figure 9: *Two sections of the solar spectrum displaying the strongest lines in the visible region (except that Ca$^+$ H at $\lambda = 3966$ Å is very similar to its doublet twin Ca$^+$ K). The lefthand segment contains the central part of the Ca$^+$ K line in the violet region of the spectrum, the righthand segment the Hα line in the red. Each segment is 30 Å (3 nm) wide. The vertical axis measures disk-averaged solar intensity so that these plots portray the solar spectrum as if it came from a non-resolved distant star. The units are erg cm^{-2} s^{-1} cm^{-1} steradian^{-1}, the same as for the Planck function defined by equation (7) on page 28. The line crowding is much larger in the violet than in the red. Most of the numerous "blends" (overlapping lines) that are superimposed on the wings of Ca$^+$ K are due to iron, an element with extraordinary rich energy level structure. The strong blend at 3944 Å is due to aluminum atoms. Very close to line center the Ca$^+$ K line displays two tiny emission peaks which betray the presence of magnetic fields in a way that is not understood. Stars that are more active than the sun have much higher peaks in their Ca$^+$ K line cores. The damping wings start just outside these peaks and extend much further than the plotted range. The Hα line in the righthand panel is much weaker. The cores of both lines are formed in the solar chromosphere, the regime where magnetic fields take over from the gas pressure in dominating solar fine structure. There are hundreds of studies (including five Utrecht PhD theses) of cool-star chromospheres using the Ca$^+$ K line core because its emission is an indicator of stellar magnetism. The Ca$^+$ K line is also much used in recent studies of solar chromospheric dynamics. The temperature sensitivity of Hα makes it complementary to Ca$^+$ K as an atmospheric diagnostic, especially of the magnetic field structures and their not-understood heating processes in the upper chromosphere. These show up as thread-like brightenings and darkenings arranged as flower petals in images taken in Hα line-center radiation. These plots are made from ASCII files of the "Kitt Peak Solar Flux Atlas" by Kurucz et al. (1984), downloaded from ftp://ftp.noao.edu/fts/fluxatl. The atlas was made with the Fourier Transform Spectrometer at Kitt Peak, a 1 m Michelson interferometer that produces unsurpassed spectral resolution ($\lambda/\Delta\lambda = 10^6$), an order of magnitude better than the "Utrecht Atlas" of the solar disk-center intensity spectrum by Minnaert et al. (1940).*

- Explain qualitatively why the solar Ca$^+$ K line is much stronger than the solar Hα line, even though hydrogen is not ionized in the solar photosphere and low chromosphere ($T \approx$

nr.	element	solar abundance	χ_1	χ_2	χ_3	χ_4
1	H	1	13.598	–	–	–
2	He	7.9×10^{-2}	24.587	54.416	–	–
6	C	3.2×10^{-4}	11.260	24.383	47.887	64.492
7	N	1.0×10^{-4}	14.534	29.601	47.448	77.472
8	O	6.3×10^{-4}	13.618	35.117	54.934	77.413
11	Na	2.0×10^{-6}	5.139	47.286	71.64	98.91
12	Mg	2.5×10^{-5}	7.646	15.035	80.143	109.31
13	Al	2.5×10^{-6}	5.986	18.826	28.448	119.99
14	Si	3.2×10^{-5}	8.151	16.345	33.492	45.141
20	Ca	2.0×10^{-6}	6.113	11.871	50.91	67.15
26	Fe	3.2×10^{-5}	7.870	16.16	30.651	54.8
38	Sr	7.1×10^{-10}	5.695	11.030	43.6	57

Table 3: Solar abundances (relative to H) and ionization energies (eV) for some elements. Mostly from Allen (1976).

$4000 - 6000$ K) where these lines are formed, and even though the solar Ca/H abundance ratio is only $N_{Ca}/N_H = 2 \times 10^{-6}$. Assume again that the observed line strength scales with the lower-level population density (which it does, although nonlinearly through a "curve of growth" as you will see in the next exercise).

- Prove your explanation by computing the expected strength ratio of these two lines as function of temperature for $P_e = 10^2$ dyne cm^{-2}. Simply combine the actual calcium ionization energies with the Schadee ad-hoc level structure. Since the Ca$^+$ K line originates from the Ca$^+$ ground state the higher levels are only needed for the partition functions and those are estimated to within a factor of two by the Schadee recipe. Therefore simply copy all your routines for Schadee's element E into routines for Ca and only adapt the ionization energies. They are given in Table 3.

- Then apply these routines as in:

```
temp=indgen(191)*100.+1000.            ; T = 1000-20000 in delta T = 100
CaH = temp                             ; declare ratio array
Caabund=2.E-6                          ; A_Ca = N_Ca / N_H
for i=0,190 do begin
  NCa = sahabolt_Ca(temp(i),1e2,2,1)
  NH = sahabolt_H(temp(i),1e2,2)
  CaH(i)=NCa*Caabund/NH
endfor
plot,temp,CaH,/ylog,$
    xtitle='temperature',ytitle='Ca II K / H alpha'
```

- Estimate the solar line strength ratio Ca$^+$ K/Hα. The temperature ranges over $T = 4000 - 6000$ K in the solar photosphere. You should get:

```
IDL> print,'Ca/H ratio at 5000~K = ',CaH(where(temp eq 5000))
Ca/H ratio at 5000~K =         7649.39
```

23

2.9 Solar Ca$^+$K versus Hα: temperature sensitivity

The two lines also differ much in their temperature sensitivity in this formation regime.

- Show this by plotting the relative population changes $(\Delta n_{\mathrm{Ca}}/\Delta T)/n_{\mathrm{Ca}}$ and $(\Delta n_{\mathrm{H}}/\Delta T)/n_{\mathrm{H}}$ for the two lower levels as function of temperature for a small temperature change ΔT:

```
   ; temperature sensitivity CaIIK and Halpha
temp=indgen(101)*100.+2000.                ; T = 2000-12000, delta T = 100
dNCadT = temp                              ; declare array
dNHdt = temp                               ; declare array
dT=1.
for i=0,100 do begin
    NCa = sahabolt_ca(temp(i),1e2,2,1)         ; Ca ion ground state
    Nca2 = sahabolt_ca(temp(i)-dT,1e2,2,1)     ; idem dT cooler
    dNCadT(i)= (NCa - NCa2)/dT/NCa             ; fractional diff quotient
    NH = sahabolt_H(temp(i),1e2,2)             ; H atom 2nd level
    NH2 = sahabolt_H(temp(i)-dT,1e2,2)         ; idem dT cooler
    dNHdT(i) = (NH-NH2)/dT/NH                  ; fractional diff quotient
endfor
plot,temp,abs(dNHdT),/ylog,yrange=[1E-5,1],$
    xtitle='temperature',ytitle='abs d n(r,s) / n(r,s)'
oplot,temp,abs(dNCadT),linestyle=2         ; Ca curve dashed
```

- Around $T = 5\,600$ K the Ca$^+$K curve dips down to very small values; the Hα curve does that around $T = 9\,500$ K. Thus, for $T \approx 5\,600$ K the temperature sensitivity of Ca$^+$K is much smaller than the temperature sensitivity of Hα. Each dip has a $\Delta n > 0$ and a $\Delta n < 0$ flank. Which is which?

- The dips can be diagnosed by overplotting the variation with temperature of each population in relative units:

```
   ; recompute as arrays and overplot relative populations
NCa=temp                                   ; declare array
NH=temp                                     ; declare array
for i=0,100 do begin
    NCa(i) = sahabolt_ca(temp(i),1e2,2,1)      ; Ca ion ground state
    NH(i) = sahabolt_H(temp(i),1e2,2)          ; H atom 2nd level
endfor
oplot,temp,NH/max(NH)
oplot,temp,NCa/max(NCa),linestyle=2        ; Ca curve again dashed
```

- Explain each flank of the two population curves and the dips in the two temperature sensitivity curves.

2.10 Hot stars versus cool stars

- Final question: find at which temperature the hydrogen in stellar photospheres with $P_{\mathrm{e}} = 10^2$ is about 50% ionized:

```
IDL> for T=2000,20000,2000 do print,T,sahabolt_H(T,1e2,1)
      2000       1.0000000
      4000       1.0000000
      6000       0.99996480
      8000       0.94991572
     10000       0.17471462
     12000      0.0096162655
     14000      0.0010102931
     16000     0.00017720948
     18000     4.4167459e-05
     20000     1.4132857e-05
```

or with a plot:

```
temp=indgen(191)*100.+1000.    ; array 1000 - 20 000 in steps 1000
nH=temp                        ; declare same size array
for i=0,190 do nH(i)=sahabolt_H(temp(i),1e2,1)
plot,temp,nH,$
   xtitle='temperature',ytitle='neutral hydrogen fraction'
```

This transition divides the "hot" from the "cool" stars. It also represents a dividing line between the mechanisms that cause the stellar continuum. In hot stars the hydrogen ionization produces so many free electrons that Thomson scattering of photons off the free electrons dominates the formation of the stellar continuum. In cool stars there are only a few free electrons, none from hydrogen but only from the ionization of elements with lower first ionization energy (Si, Fe, Al, Mg, Ca, Na; see Table 3). Interactions between these rare free electrons and the abundant neutral hydrogen atoms, momentarily combining into "H-minus ions", then dominate the formation of the stellar continuum.

3 Fraunhofer line strengths and the curve of growth ("Marcel Minnaert")

In Exercise 1 you re-invented the Harvard spectral classification in order to typecast stellar spectra morphologically. In Exercise 2 you interpreted the Harvard classification in terms of physics by using the Saha and Boltzmann laws for the partitioning of the particles of an element over its various modes of existence. The strength variations of spectral lines along the main sequence were found to be primarily due to change in temperature.

We have not yet answered the question yet *how* spectral lines form. This issue is addressed here following Minnaert's work at Utrecht between World Wars I and II. This exercise introduces you to some of the basic concepts introduced by Minnaert. They are still in use and are instructive to re-develop yourself.

Figure 10: Marcel G.J. Minnaert (Brugge 1893 — Utrecht 1970) was a Flemish biologist who became a physicist at Utrecht after World War I, picking up W.H. Julius' interest in solar spectroscopy and taking over the solar physics department after Julius' death in 1925. In 1937 Minnaert succeeded A.A. Nijland as director of "Sterrewacht Sonnenborgh" and revived it into a spectroscopy-oriented astrophysical institute. In addition, he was a well-known physics pedagogue. His three books "De natuurkunde van het vrije veld" (Outdoors Physics) are a delightful guide to outdoors physics phenomena. I took this photograph in 1967.

3.1 The Planck law

For electromagnetic radiation the counterparts to the material Saha and Boltzmann distributions are the Planck law and its relatives (the Wien displacement law and the Stefan-Boltzmann law)[9]. They also hold strictly in TE ('Thermodynamical Equilibrium") and reasonably well in stellar photospheres. The Planck function specifies the radiation intensity emitted by a gas or a body

---

[9]The Saha and Boltzman (and also the Maxwell) distributions have $\exp(-E/kT)$ without the -1 that is present in the denominator of the Planck function. The reason for this difference is a basic one: atoms, ions and electrons are fermions that cannot occupy the same space-time-impulse slot, but photons are bosons that actually prefer to share places, as in a laser.

in TE (a "black body") as:

$$B_\lambda(T) = \frac{2hc^2}{\lambda^5} \frac{1}{\mathrm{e}^{hc/\lambda kT} - 1} \tag{7}$$

with h the Planck constant, c the speed of light, k the Boltzmann constant, λ the wavelength and T the temperature. The dimension of B_λ in the cgs units used here is $\mathrm{erg\,cm^{-2}\,s^{-1}\,cm^{-1}\,steradian^{-1}}$ (in standard units $\mathrm{W\,m^{-2}\,m^{-1}\,steradian^{-1}}$), which is the dimension of radiative intensity in a specific direction[10].

- Write an IDL function `PLANCK,TEMP,WAV` in cgs units. The required constants are given in Table 2 on page 14. For `TEMP=5000` and `WAV=5000E-8` (5000 Ångstrom, in the yellow part of the visible wavelength region and at about the sensitivity peak of your eyes) it should give:

```
IDL> .com planck
% Compiled module: PLANCK.
IDL> print,planck(5000,5000E-8)
    1.2107502e+14
```

- Use it to plot Planck curves against wavelength in the visble part of the spectrum for different stellar-like temperatures, for example with the following statements in a main IDL file `SSA3.PRO`:

```
wav=indgen(100)*200.+1000.    ; produces wav(0,...99) = 1000 - 20800
print,wav                      ; check that
b=wav                          ; declare float array of the same size
for i=0,99 do b(i)=planck(8000,wav(i)*1E-8)
plot,wav,b,xtitle='wavelength (Angstrom)',ytitle='Planck function',$
  xmargin=[15,5],$             ; otherwise no place for y-axis label
  charsize=1.2                 ; bigger characters
for T=8000,5000,-200 do  begin    ; step from 8000 K down to 5000 K
  for i=0,99 do b(i)=planck(T,wav(i)*1E-8)
  oplot,wav,b        ; overplots extra curves in existing graph
endfor               ; begin...end sequences can't go on command line
```

- Study the Planck function properties. $B_\lambda(T)$ increases at any wavelength with the temperature, but much faster (exponentially, Wien regime) at short wavelengths then at long wavelengths (linearly, Rayleigh-Jeans regime). The peak divides the two regimes and shifts to shorter wavelengths for higher temperature (Wien displacement law). The spectrum-integrated Planck function (area under the curve in this linear plot) increases steeply with temperature (Stefan-Boltzmann law).

- Add `,/ylog` to the `plot` statement to make the y-axis logarithmic. Inspect the result. Then make the x-axis also logarithmic and inspect the result. Explain the slopes of the righthand part.

---

[10]The quadratic length dimension ($\mathrm{cm^{-2}}$) represents a measurement area oriented perpendicular to the beam direction. The linear length dimension ($\mathrm{cm^{-1}}$) represents the spectral bandwidth ($\Delta\lambda = 1\,\mathrm{cm}$). It becomes $\Delta\nu = 1\,\mathrm{Hz}$ for B_ν in frequency units. Steradians measure beam spreading over solid angle (a wedge of a sphere), just as radians measure planar angles (a wedge of a circle). Sometimes B_λ is defined as *flux*, the energy radiated outward by a surface, without $\mathrm{steradian^{-1}}$ and a factor π larger.

3.2 Radiation through an isothermal layer

We need another quantity next to the radiation produced by a gas of temperature T, namely the amount of absorption. Take the situation sketched in Figure 11. A beam of radiation with intensity $I(0)$ passes through a layer in which it is attenuated. The weakened intensity that emerges on the right is given by

$$I = I(0)\,\mathrm{e}^{-\tau}, \tag{8}$$

in which the decay parameter τ specifies the attenuation by absorption in the layer. It is a dimensionless measure of the opaqueness that is usually called the "optical thickness" because it measures how thick the layer is, not in cm but in terms of its effect on the passing radiation. Nothing comes through if $\tau \gg 1$ and (almost) everything comes through if $\tau \ll 1$.
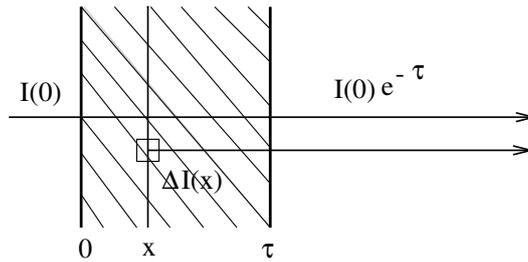

Figure 11: Radiation through a layer. The incident intensity at the left is attenuated by absorption in the layer as specified by its total opaqueness τ (the "optical thickness" of the layer). The internal production of radiation $\Delta I(x)$ in a thin sublayer with thickness Δx that is added to the beam locally is given by the product of the Planck function $B[T(x)]$ and the sublayer opaqueness $\Delta\tau(x)$; this contribution is then attenuated by the remainder of the layer.

The next step is to add the radiation that originates within the layer itself. Its amount is locally equal to $\Delta I = B_\lambda(T)\,\Delta\tau$. The scaling with $\Delta\tau$ comes in through a Kirchhoff law which says that a medium radiates better when it absorbs better (a "black" body radiates stronger than a white one). This local contribution at a location x within the layer is subsequently attenuated by the remainder of the layer to the right, so that its addition to the emergent beam is given by:

$$\Delta I_\lambda = B_\lambda[T(x)]\,\Delta\tau(x)\;\mathrm{e}^{-(\tau-\tau(x))}. \tag{9}$$

The total emergent intensity is:

$$I_\lambda = I_\lambda(0)\,\mathrm{e}^{-\tau} + \int_0^\tau B_\lambda[T(x)]\;\mathrm{e}^{-(\tau-\tau(x))}\,\mathrm{d}\tau(x) \tag{10}$$

which for an isothermal layer (T and therefore also $B_\lambda(T)$ independent of x) simplifies to:

$$I_\lambda = I_\lambda(0)\,\mathrm{e}^{-\tau} + B_\lambda\left(1 - \mathrm{e}^{-\tau}\right). \tag{11}$$

- Derive (11) from (10).

- Make plots of the emergent intensity I_λ for given values B_λ and $I_\lambda(0)$ against τ:

```
B=2.
tau=indgen(101)/10.+0.01      ; set array tau = 0.01-10 in steps 0.01
int=tau                       ; declare float array of the same size
for I0=4,0,-1 do begin        ; step down from I0=4 to I0=0
  for i=0,100 do int(i)=I0 * exp(-tau(i)) + B*(1-exp(-tau(i)))
  if i0 eq 4 then plot,tau,int,$
      xtitle='tau',ytitle='Intensity',charsize=1.3
  if i0 ne 4 then oplot,tau,int
endfor
```

- How does I_λ depend on τ for $\tau \ll 1$ when $I_\lambda(0) = 0$ (add `,/xlog,/ylog` to study the behavior at small τ)? And when $I_\lambda(0) > B_\lambda$? Such a layer is called "optically thin", why?

- A layer is called "optically thick" when it has $\tau \gg 1$. Why? The emergent intensity becomes independent of τ for large τ. Can you explain why this is so in physical terms?

3.3 Spectral lines from a solar reversing layer

We will now apply the above result for an isothermal layer to a simple model in which the Fraunhofer lines in the solar spectrum are explained by a "reversing layer". Cecilia Payne had this model in mind when she plotted her Saha-Boltzmann population curves. She thought that her curves described the local density of the line-causing atoms and ions within stellar reversing layers.
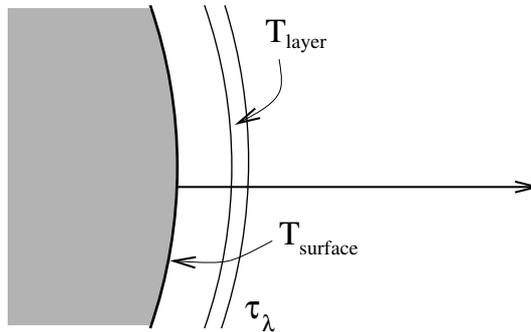

Figure 12: *The Schuster-Schwarzschild or reversing-layer model. The stellar surface radiates an intensity given by $B_\lambda(T_{\mathrm{surface}})$. The shell around the surface only affects this radiation at the wavelengths where atoms provide a bound-bound transition between two discrete energy levels. These spectral line transitions cause attenuation τ_λ. The layer has temperature T_{layer} and gives a thermal contribution $B_\lambda(T_{\mathrm{layer}}) [1 - \exp(-\tau_\lambda)]$ as in Eq. (11).*

Schuster-Schwarzschild model. The basic assumptions are that the continuous radiation, without spectral lines, is emitted by the stellar surface and irradiates a separate layer with the intensity

$$I_\lambda(0) = B_\lambda(T_{\mathrm{surface}}), \tag{12}$$

and that this layer sits as a shell around the star and causes attenuation and local emission *only* at the wavelengths of spectral lines. Thus, the shell is thought to be made up exclusively by line-causing atoms or ions.

30

The star is optically thick (any star is optically thick!) so that its surface radiates with the $\tau \gg 1$ solution $I_\lambda = B_\lambda(T_{\text{surface}})$ of (11), but the shell may be optically thin or thick at the line wavelength depending on the atom concentration. The line-causing atoms in the shell have temperature T_{layer} so that the local production of radiation in the layer at the line wavelengths is given by $B_\lambda(T_{\text{layer}}) \Delta\tau(x)$. The emergent radiation at the line wavelengths is then given by (11) and (12) as:

$$I_\lambda = B_\lambda(T_{\text{surface}}) \, e^{-\tau_\lambda} + B_\lambda(T_{\text{layer}}) \, (1 - e^{-\tau_\lambda}). \tag{13}$$

Voigt profile. The opaqueness τ in (13) has gotten an index λ because it varies over the spectral line. When atoms absorb or emit a photon at the energy at which the valence electron may jump between two bound energy levels (bound electron orbits), the effect is not limited to an infinitely sharp delta function at λ with $hc/\lambda = \chi_{r,s} - \chi_{r,t}$ but it is a little bit spread out in wavelength. An obvious cause for such "line broadening" consists of the Doppler shifts given by individual atoms due to their thermal motions. Other broadening is due to Coulomb interactions with neighboring particles. This broadening distribution is described by

$$\tau(u) = \tau(0) \, V(a, u) \tag{14}$$

where V is called the Voigt function and u measures the wavelength separation $\Delta\lambda = \lambda - \lambda(0)$ from the center of the line at $\lambda = \lambda(0)$ in dimensionless units

$$u \equiv \Delta\lambda/\Delta\lambda_{\text{D}}, \tag{15}$$

where $\Delta\lambda_{\text{D}}$ is the "Doppler width" defined as

$$\Delta\lambda_{\text{D}} \equiv \frac{\lambda}{c}\sqrt{2kT/m} \tag{16}$$

with m the mass of the line-causing particles (for example iron with $m_{\text{Fe}} \approx 56\,m_{\text{H}} \approx 9.3 \times 10^{-23}$ g). The parameter a in (14) measures the amount of Coulomb disturbances (called "damping"). Stellar atmospheres typically have $a \approx 0.01 - 0.5$. The Voigt function $V(a, u)$ is defined as:

$$V(a, u) \equiv \frac{1}{\Delta\lambda_{\text{D}}\sqrt{\pi}} \frac{a}{\pi} \int_{-\infty}^{+\infty} \frac{e^{-y^2}}{(u-y)^2 + a^2} \, dy. \tag{17}$$

It represents the convolution (smearing) of a Gauss profile with a Lorentz profile and therefore has a Gaussian shape close to line center ($u = 0$) due to the thermal Doppler shifts ("Doppler core") and extended Lorentzian wings due to disturbances by other particles ("damping wings"). A reasonable approximation is obtained by taking the sum rather than the convolution of the two profiles:

$$V(a, u) \approx \frac{1}{\Delta\lambda_{\text{D}}\sqrt{\pi}} \left[e^{-u^2} + \frac{a}{\sqrt{\pi}\,u^2} \right]. \tag{18}$$

- Start the IDL Online Help by typing ? on the command line. Inspect the description of the VOIGT(a,u) function. We might have programmed approximation (18), but since IDL furnishes the real thing we will use that instead.

- Plot the Voigt function against u from $u = -10$ to $u = +10$ for $a = 0.1$:

```
u=indgen(201)/10.-10.                    ; u = -10 to 10 in 0.1 steps
vau=u                                    ; declare same-size array
a=0.1                                    ; damping parameter
for i=0,200 do vau(i)=VOIGT(a,abs(u(i))) ; taking abs corrects IDL errors
plot,u,vau,yrange=[0,1]                  ; yrange fixed to compare plots
```

- Cursor back up and vary the value of a between $a = 1$ and $a = 0.001$ to see the effect of this parameter. Also add `,/ylog` (without setting `yrange`) to inspect the far wings of the profile. Use approximation (18) to explain what you see.

Emergent line profiles. You are now able to compute and plot stellar spectral line profiles by combining (13) with (14). Again use the dimensionless u units for the wavelength scale so that you don't have to evaluate the Doppler width $\Delta\lambda_{\mathrm{D}}$.

- Write an IDL sequence that computes Schuster-Schwarzschild line profiles. Take $T_{\mathrm{surface}} = 5700$ K, $T_{\mathrm{layer}} = 4200$ K, $a = 0.1$, $\lambda = 5000$ Å. These values are good choices for the solar photosphere as seen in the optical part of the spectrum. First plot a profile I against u for $\tau(0) = 1$:

```
Ts=5700                  ; solar surface temperature
Tl=4200                  ; solar T-min temperature = 'reversing layer'
a=0.1                    ; damping parameter
wav=5000.D-8             ; wavelength in cm
tau0=1                   ; reversing layer thickness at line center
u=indgen(201)/10.-10.    ; u = -10 to 10 in 0.1 steps
int=u                    ; declare array
for i=0,200 do begin
   tau=tau0 * VOIGT(a,abs(u(i)))
   int(i)=PLANCK(Ts,wav) * exp(-tau) + PLANCK(Tl,wav)*(1.-exp(-tau))
endfor
plot,u,int
```

- Study the appearance of the line in the spectrum as a function of $\tau(0)$ over the range $\log\tau(0) = -2$ to $\log\tau(0) = 2$. Example:

```
tau0=[0.01, 0.05, 0.1, 0.5, 1, 5, 10, 50, 100]
for itau=0,8 do begin
  for i=0,200 do begin
    tau=tau0(itau) * VOIGT(a,abs(u(i)))
    int(i)=PLANCK(Ts,wav) * exp(-tau) + PLANCK(Tl,wav)*(1.-exp(-tau))
  endfor
  oplot,u,int
endfor
```

- How do you explain the profile shapes for $\tau(0) \ll 1$?

- Why is there a low-intensity saturation limit for $\tau \gg 1$?

- Why do the line wings develop only for very large $\tau(0)$?

- Where do the wings end?

- For which values of $\tau(0)$ is the layer optically thin, respectively optically thick, at line center? And at $u = 5$?

- Now study the dependence of these line profiles on wavelength by repeating the above for $\lambda = 2000$ Å (ultraviolet) and $\lambda = 10\,000$ Å (near infrared). What sets the top value I_{cont}

and the limit value reached at line center by $I(0)$? Check these values by computing them directly on the command line. What happens to these values at other wavelengths?

- Observed spectra that are measured in detector counts without absolute intensity calibration (as in your Clea-Spec data gathering in Exercise 1) are usually scaled to the local continuum intensity by plotting $I_\lambda/I_{\text{cont}}$ against wavelength. Do that for the above profiles at the same three wavelengths:

```
for iwav=1,3 do begin
  wav=(iwav^2+1)*1.D-5              ; wav = 2000, 5000, 10000 Angstrom
  for itau=0,8 do begin
    for i=0,200 do begin
      tau=tau0(itau) * VOIGT(a,abs(u(i)))
      int(i)=PLANCK(Ts,wav) * exp(-tau) + PLANCK(Tl,wav)*(1.-exp(-tau))
    endfor
    int=int/int(0)                  ; convert into relative intensity
    if iwav eq 1 and itau eq 0 then plot,u,int
    if iwav eq 1 and itau gt 0 then oplot,u,int
    if iwav eq 2 then oplot,u,int,linestyle=1        ; dotted
    if iwav eq 3 then oplot,u,int,linestyle=4        ; dash dot dot dot
  endfor
endfor
```

- Explain the wavelength dependences in this plot.

3.4 The equivalent width of spectral lines

Your profile plots demonstrate that the growth of the absorption feature in the spectrum for increasing $\tau(0)$ is faster for small $\tau(0)$ then when it "saturates" for larger $\tau(0)$. Minnaert and coworkers introduced the *equivalent width* W_λ as a line-strength parameter to measure this growth quantitively. It measures the integrated line depression in the normalized spectrum:

$$W_\lambda \equiv \int \frac{I_{\text{cont}} - I(\lambda)}{I_{\text{cont}}} \, \mathrm{d}\lambda \tag{19}$$

so that its value is the same as the width of a rectangular piece of spectrum that blocks the same amount of spectrum completely (Figure 13). We will express it here in the dimensionless wavelength units u.

- In order to add such profile integration it becomes handy to turn the profile computation into an IDL function PROFILE(a,tau0,u):
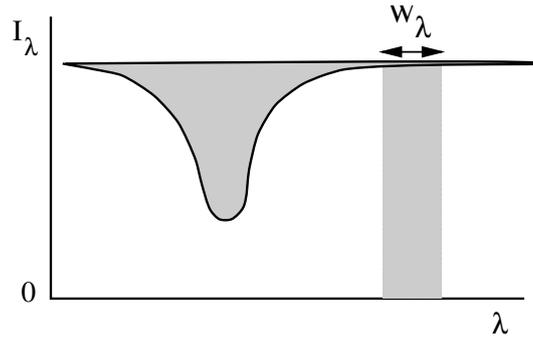
Figure 13: The equivalent width of a spectral line is the width of a rectangular piece of fully blocked spectrum with the same spectral area as the integrated line depression.

```
function profile,a,tau0,u
  ; return a Schuster-Schwarzschild profile
  ; input: a = damping parameter
  ;        tau0 = SS layer thickness at line center
  ;        u = wavelength array in Doppler units
  ; output: int = intensity array
Ts=5700
Tl=4200
wav=5000.E-8
int=u
usize=SIZE(u)              ; IDL SIZE returns array type and dimensions
for i=0,usize(1)-1 do begin
   tau=tau0 * VOIGT(a,abs(u(i)))
   int(i)=PLANCK(Ts,wav)*exp(-tau) + PLANCK(Tl,wav)*(1.-exp(-tau))
endfor
return,int
end
```

- Check your routine:
```
u=indgen(1001)/2.5-200.          ; u = -200 to +200 in steps of 0.4
a=0.1
tau0=1e2
int=profile(a,tau0,u)
plot,u,int
```

- Continue by computing the equivalent width with the IDL TOTAL function (check it out in the Online Help):
```
reldepth=(int(0)-int)/int(0)   ; line depth in relative units
plot,u,reldepth
eqw=total(reldepth)*0.4         ; integral = TOTAL times interval
print,eqw
```

The wide range of u specified above is needed to fully accommodate the extended line wings that develop at large $\tau(0)$, otherwise int(0) will not equal I_{cont}. However, the sampling should be finely spaced around line center to get the proper summation for narrow lines at small $\tau(0)$.

34

Spectral line codes therefore often use equidistant wavelength spacing over the Doppler core but logarithmic wavelength spacing in the damping wings.
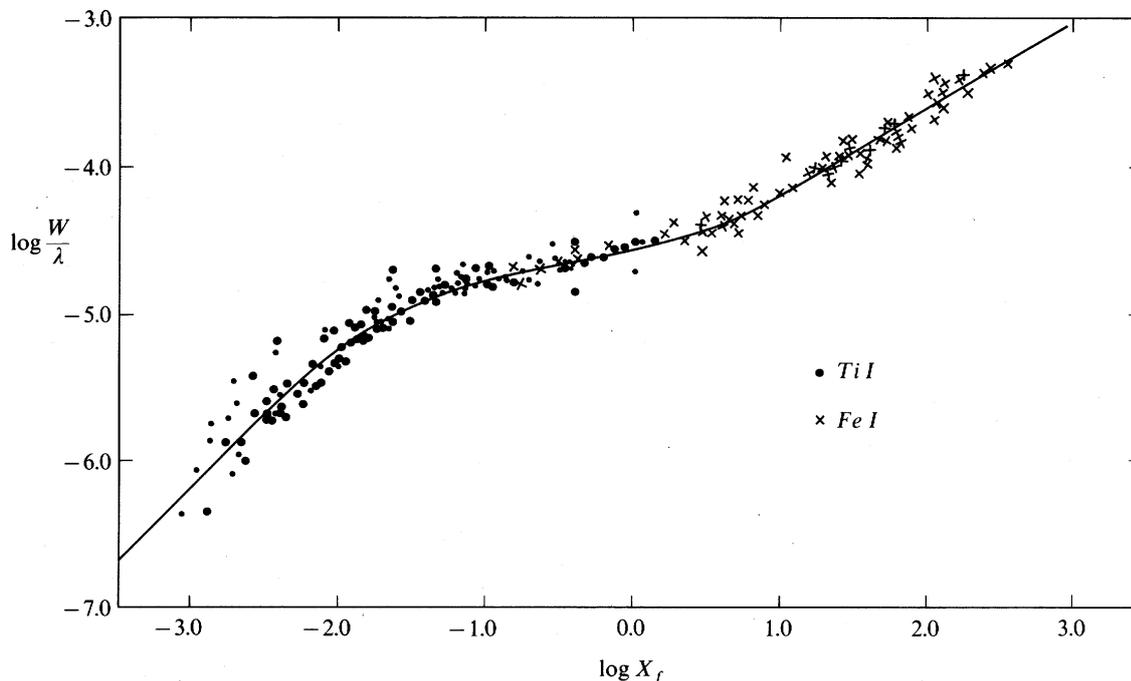

Figure 14: *Empirical curve of growth for solar Fe I and Ti I lines. Taken from Mihalas (1970) who took it from Wright (1948). Wright measured the equivalent widths of 700 lines in the Utrecht Atlas. The quantity X_f along the x axis scales with the product of the transition probability and the population density of the lower level of each line. The populations were computed from the Saha-Boltzmann laws as in Exercise 2. The transition probabilities were measured in the laboratory. The normalization of W by λ removes the λ-dependence of the Doppler width defined by (16).*

3.5 The curve of growth

The idea behind the equivalent width was obviously that the amount of spectral blocking should be a direct measure of the number of atoms in the reversing layer. They should set the opaqueness $\tau(0)$ of the layer. Your profile plots illustrate that the profile growth is only linear with $\tau(0)$ for $\tau(0) \ll 1$. The "curve of growth" describes the full dependence: the growth of the line strength with the line-causing particle density. Figure 14 shows an observed example.

- Compute and plot a curve of growth by plotting $\log W_\lambda$ against $\log \tau(0)$:

```
tau0=10^(indgen(61)/10.-2.)  ; 10^-2 to 10^4, 0.1 steps in the log
eqw=tau0                     ; same size array
for i=0,60 do begin
  int=profile(a,tau0(i),u)
  reldepth=(int(0)-int)/int(0)
  eqw(i)=total(reldepth)*0.4
endfor
plot,tau0,eqw,xtitle='tau0',ytitle='equivalent width',/xlog,/ylog
```

- Explain what happens in the three different parts.

- The first part has slope 1:1, the third part has slope 1:2 in this log-log plot. Why?

- Which parameter controls the location of the onset of the third part? Give a rough estimate of its value for solar iron lines through comparison with Figure 14.

- Final question: of which parameter should you raise the numerical value in order to produce emission lines instead of absorption lines? Change it accordingly and rerun your programs to produce emission profiles and an emission-line curve of growth. Avoid plotting negative W_λ values logarithmically by:

```
plot,tau0,abs(eqw),$
    xtitle='tau0',ytitle='abs(equivalent width)',/xlog,/ylog
```

Epilogue

In these three exercises "Stellar Spectra A" you have quickly gone through half a century of stellar spectroscopy (the first half of the twentieth century), ending with a model of spectral line formation that roughly explains the strengths and shapes of solar line profiles. Combination of this model with Saha-Boltzmann routines as in Exercise 2 explains stellar spectra throughout the Hertzsprung-Russell diagram. However, the model is very simple. Its two major deficiencies are:

- use of the single-layer Schuster-Schwarschild description (Exercise 3).

  It is obviously unrealistic to stick all line-causing particles together in a separate layer. The gas in a stellar atmosphere is well mixed; the gas particles contribute to local absorption and emission with continuum-causing processes and line-causing processes at the same time. A much better description is therefore to have say a hundred layers instead of a single one, each with its own $\tau^c(i)$ for the continuum and additional $\tau^l(i)$ for the spectral line. If the temperature $T(i)$ is then set to smoothly decline outwards, a fairly realistic model of a stellar atmosphere results.

  Setting the ratio τ^l/τ^c constant for all i would make this many-layer model a "Milne-Eddington" atmosphere, a much better description than the Schuster-Schwarzschild one.

  Computing $\tau^c(i)$ and $\tau^l(i)$ in detail from the Saha-Boltzmann laws would make it an "LTE model atmosphere", where the "Local" in LTE = Local Thermodynamic Equilibrium alludes to using the local temperature within a stratified atmosphere in the TE laws. Such local-equilibrium modeling has been used for stellar abundance determination throughout the second half of the twentieth century. It is treated in exercises "Stellar Spectra B: LTE line formation".

- use of the TE partitioning laws (Exercises 2 and 3).

  We have assumed that the temperature defines both the particle populations (Saha and Boltzmann laws; Exercise 2) and the production of radiation (Planck law; Exercise 3). These TE laws are accurate in the stellar interior and hold reasonably well in the deeper parts of a stellar atmosphere, but not in the outer parts. For example, they do not hold at all in the solar corona. Its high temperature ($T_e \approx 2 \times 10^6$ K) and low density ($N_e \approx 10^6$ cm^{-3}) cause ionization to very high stages but without reaching thermodynamical equilibrium because the X-ray radiation from the ions escapes directly from the corona and represents a limiting energy loss. As a result, the production of coronal radiation falls very far below the coronal Planck function, and the ion populations are far below the Saha prediction.

  The TE laws hold much better for the stellar photospheres from which the visible radiation escapes. Although that radiation leak contributes most of the total stellar energy loss, it represents only a tiny loss in comparison to the local photospheric thermal energy content. LTE is therefore a reasonable assumption for many photospheric lines and continua — but by no means for all and certainly not for chromospheric lines such as Ca$^+$K and Hα in the solar spectrum. Exercises "Stellar Spectra C: NLTE line formation" treat techniques appropriate to those.

References

Abt, H. A., Meinel, A. B., Morgan, W. W., and Tapscott, J. W.: 1968, *An Atlas of Low-Dispersion Grating Stellar Spectra*, Kitt Peak National Observatory, Tucson, USA

Allen, C. W.: 1976, *Astrophysical Quantities*, Athlone Press, Univ. London

De Jager, C., Schadee, A., Svestka, Z., Van Tend, W., Machado, M. E., Strong, K. T., and Woodgate, B. E.: 1983, *Solar Phys.* **84**, 205

Hearnshaw, J. B.: 1986, *The analysis of starlight. One hundred and fifty years of astronomical spectroscopy*, Cambridge Univ. Press, Cambridge UK

Kurucz, R. L., Furenlid, I., Brault, J. W., and Testerman, L.: 1984, *Solar Flux Atlas from 296 to 1300 nm*, NSO Atlas Nr. 1, National Solar Observatory, Sunspot, New Mexico

Mihalas, D.: 1970, *Stellar Atmospheres*, W. H. Freeman and Co., San Francisco (first edition)

Minnaert, M. G. J., Mulders, G. F. W., and Houtgast, J.: 1940, *Photometric Atlas of the Solar Spectrum 3332 Å to 8771 Å*, Schnabel, Amsterdam

Moore, C. E., Minnaert, M. G. J., and Houtgast, J.: 1966, *The Solar Spectrum 2935 Å to 8770 Å. Second Revision of Rowland's Preliminary Table of Solar Spectrum Wavelengths*, NBS Monograph 61, National Bureau of Standards, Washington

Novotny, E.: 1973, *Introduction to stellar atmospheres and interiors*, Oxford Univ. Press, New York

Payne, C. H.: 1924, *Harvard Circular* **256**, 1

Payne, C. H.: 1925, *Stellar Atmospheres*, Harvard Observatory Monographs No. 1, Cambridge, Mass.

Rybicki, G. B. and Lightman, A. P.: 1979, *Radiative Processes in Astrophysics*, John Wiley & Sons, Inc., New York

Schadee, A.: 1964, *The Formation of Molecular Lines in the Solar Spectrum*, PhD Thesis, Utrecht University

Schadee, A.: 1978, *J. Quant. Spectrosc. Radiat. Transfer* **19**, 517

Wright, K. O.: 1948, *Pub. Dominion Astrophys. Obs.* **8**, 1